University of Wollongong
Research Online

Faculty of Engineering - Papers (Archive)

Faculty of Engineering and Information Sciences

2001

Pyrite Oxidation Model for Assessing Ground-Water Management Strategies in Acid Sulfate Soils

B. Blunden
University of Wollongong

Buddhima Indraratna
University of Wollongong, buddhima_indraratna@uow.edu.au

Publication Details

This article was originally published as: Blunden, B & Indraratna, B, Pyrite Oxidation Model for Assessing Ground-Water Management Strategies in Acid Sulfate Soils, Journal of Geotechnical and Geoenvironmental Engineering, 2001, 127(2), 146-157. Copyright American Society of Civil Engineers. Original journal available here.

Research Online is the open access institutional repository for the University of Wollongong. For further information contact the UOW Library: research-pubs@uow.edu.au

Pyrite Oxidation Model for Assessing Ground-Water Management Strategies in Acid Sulfate Soils

By B. Blunden[1] and B. Indraratna,[2] Member, ASCE

Abstract: A theoretical approach for calculating pyrite oxidation in acid sulfate soil with a macropore/matrix structure is described. This approach accounts for vertical oxygen transport through soil macropores and the subsequent lateral diffusion of oxygen into the soil matrix. As oxygen is supplied into the matrix, it is consumed by pyrite and other oxygen-consuming processes. A numerical solution to the theoretical model was developed and used in the computer simulation model ACID3D. The numerical approach is based on a linear relationship between oxygen consumption and dissolved oxygen concentration. The numerical scheme is shown to be in good agreement with the analytical solutions. ACID3D was used in conjunction with a commercially available saturated/unsaturated water flow model to assess the effectiveness of a ground-water management strategy to minimize acid generation caused by pyrite oxidation currently being carried out on a trial site on the south coast of New South Wales, Australia.

INTRODUCTION

Acid sulfate soil is the common name given to coastal floodplain deposits (mainly silty clays) containing oxidizable, or partly oxidized, sulfide minerals. The general form of these sulfide minerals is cubic iron pyrite (FeS_2) although other forms of sulfide compounds can also exist in small concentrations (Bush and Sullivan 1999). Where acid sulfate soils remain in a reduced condition, the sulfides remain chemically inert. Pyrite oxidizes when it is exposed to atmospheric oxygen, which results in the formation of acidic oxidation products, namely Fe^{2+}, SO_4^{2-}, and H^+. Concrete bridge piers, culverts, and foundations are subject to sulfate attack under these conditions, and the use of sulfate-resistant concrete is now recommended in many parts of the New South Wales (NSW) coastline for the construction of public infrastructure. Under acidic conditions, Fe^{2+} is soluble and can be transported into streams at a considerable distance from the source of pyrite (Nyguyen and Wilander 1995). In water, Fe^{2+} oxidizes to Fe^{3+}, which precipitates as ferrihydrite (FeOOH), the characteristic red-brown floc, and a further 2 mol of acid, which contributes to environmental degradation (Sammut et al. 1996). The Fe^{2+} oxidation reaction consumes oxygen from water and can be associated with low dissolved oxygen concentrations in streams. In addition, the acidic leachate discharged from the oxidized acid sulfate soil contains very high concentrations of dissolved metals such as Al^{3+}, which can be toxic to aquatic organisms.

In Australia, deep surface drains installed in coastal lowlands contribute to the unrestricted discharge of acidic oxidation products from acid sulfate soils. The generation and transport of acid produced form the oxidation of pyrite in sulfidic sediments is largely determined by the shallow ground-water hydrology of the catchment. Where the ground-water table falls below the elevation of the acid sulfate soil layer, atmospheric oxygen is able to diffuse through the overlying soil pores to react with the sulfide minerals in the acid sulfate soils to generate acid.

Flood mitigation drains have one-way flap valves where the flap valves discharge water from the drain into the nearby creek at low tide, but prevents entry of water from the creek into the drain at high tide. This ensures that the water level in the drain quickly reaches a steady-state elevation at the low tide level. Given the steady-state water level in the drain, a hydraulic gradient from the surrounding land toward the drain is established, which causes a general lowering of the ground-water elevation in the surrounding catchment. Pyrite may be exposed to oxidizing conditions where drawdown has caused the ground-water table to fall below or into the acid sulfate soil layer. If low rainfall conditions prevail, evapotranspiration from the ground water can lower the ground-water table even further to cause a hydraulic gradient where water flows away from the drain. In most acid sulfate soils, the hydraulic conductivity is smaller than the evapotranspirative loss from the ground-water table, giving rise to substantial lowering of the ground-water table away from the drain. Under these dry climatic conditions, very large volumes of acid sulfate soil can be exposed to oxidizing conditions. Once the ground water is recharged by rainfall, the acidic oxidation products already generated when the ground-water table was below the acid sulfate soil layer can then be entrained into the ground water and transported to the drains. The legacy of previously constructed drainage works that discharge large quantities of acid into coastal waterways remains a major environmental, economic, and social problem that requires urgent attention in low-lying coastal areas of NSW, Australia.

Simulation of Pyrite Oxidation and Distribution of Acidic Products

The amount of acidic pyrite oxidation product generated at a site, or the effectiveness of potential acid sulfate soil-management techniques that rely on better management of the ground-water table, can be assessed by using simulation models that consider the ground-water hydrology at a site and its relationship to oxidation of pyrite. Considerable effort has been placed into the development of analytical and numerical solutions for modeling the oxidation of pyrite or other similar sulfidic minerals [e.g., Elberling et al. (1994), Jaynes et al. (1984), Wunderly et al. (1996)]. Development of these models has generally focused on better understanding the generation of acidic leachate from waste rock dumps and tailings lagoons associated with sulfidic mineral mining activities, and as such, are only partly applicable to the study of acid sulfate soils. In most models that simulate pyrite oxidation in pyritic waste rock dumps, entry of oxygen is simulated as a diffusion front through a uniform, structureless media. This is not characteristic of many acid sulfate soils where oxygen transport to the pyritic sediments is dominated by preferential flow through

[1]PhD Candidate, Facu. of Engrg., Univ. of Wollongong, NSW 2522, Australia.

[2]Prof. of Civ. Engrg., Facu. of Engrg., Univ. of Wollongong, NSW 2522, Australia.

Note. Discussion open until July 1, 2001. To extend the closing date one month, a written request must be filed with the ASCE Manager of Journals. The manuscript for this paper was submitted for review and possible publication on July 7, 1999. This paper is part of the ***Journal of Geotechnical and Geoenvironmental Engineering***, Vol. 127, No. 2, February, 2001. ©ASCE, ISSN 1090-0241/01/0002-0146–0157/$8.00 + $.50 per page. Paper No. 21331.

macropores. Only one pyrite oxidation model has been designed specifically for the simulation of acid generation and transport in acid sulfate soils (Bronswijk et al. 1993). However, this model only simulates oxygen transport and pyrite oxidation in one dimension.

Blunden and Indraratna (2000) showed that the magnitude and distribution of pyrite oxidation in land underlain by acid sulfate soil was not spatially or temporally uniform. In order to assess the effectiveness of ground-water management strategies at the appropriate spatial scale (e.g., paddock or subcatchment), Blunden and Indraratna (2000) recommended that the modeling of pyrite oxidation and the subsequent generation of sulfuric acid should be carried out in 2D or 3D space. This enables the magnitude and distribution of pyrite oxidation to be assessed over a site with reference to changes in the ground-water regime that are influenced by deep flood mitigation drains.

A 3D pyrite oxidation numerical model suitable for the assessment of acid sulfate soil-management strategies at the subcatchment scale is described in this paper. The value of assessing pyrite oxidation across the site is shown with reference to the simulation of a drained site, i.e., existing deep flood mitigation drains with flap valve floodgates, and a scenario with elevated drain water levels.

THEORETICAL FORMULATIONS FOR PYRITE OXIDATION MODEL

Downward Oxygen Transport through Macropores

The oxidation of pyrite in acid sulfate soils is largely determined by the concentration of oxygen in the soil. The concentration of oxygen at a particular depth in the soil determines the rate of pyrite oxidation at that depth (Dent 1986). Other factors of secondary nature such as the oxidation of pyrite by reducing Fe^{3+} have been neglected. The oxygen consumption at any depth is dependent upon:

- The diffusion of oxygen into the soil
- The consumption of oxygen in the soil

Refsgaard et al. (1991) described this relationship between oxygen concentration, supply, and consumption as

$$\frac{\partial n_e C_a(x)}{\partial t} = \frac{\partial}{\partial x}\left(D_s(n_e)\,\frac{\partial C_a(x)}{\partial x}\right) - \alpha_v \qquad (1)$$

where $C_a(x)$ = concentration of oxygen in air-filled pores (m^3/unit volume of soil); D_s = diffusion coefficient of oxygen in air-filled pores (m^2 day^{-1}); t = time (days); x = distance (m); n_e = air-filled porosity; and α_v = volumetric consumption rate of oxygen/day.

Eq. (1) is difficult to solve analytically due to the heterogeneity of porosity down a soil profile, the dependence of D_s on the air-filled pore space, and the influence of the oxygen consumption rate. However, (1) can be simplified by assuming that the steady-state oxygen concentration profile forms quickly, say, within minutes or hours. Where the oxygen concentration profile in the soil is calculated on a daily time step (i.e., at a steady state) then (1) simplifies to

$$\frac{\partial}{\partial x}\left(D_s(n_e)\,\frac{\partial C_a(x)}{\partial x}\right) = \alpha_v \qquad (2)$$

where the diffusion of oxygen from the atmosphere is equal to the consumption of oxygen within the soil.

Soil Structure

The physical structure of the acid sulfate and the overlying soil layers largely determine D_s. For the acid sulfate soils encountered at the authors' field site and elsewhere in Australia [e.g., Wilson et al. (1999)], the most outstanding structural feature of the soil is the presence of large (2–10 mm diameter), continuous, and straight macropores created by previous plant root activity. Roots of growing plants are confined to the upper 0.5 m top soil horizon of the profile where acidity and dissolved aluminum do not restrict root exploration. The older macropore channels within the clayey matrix at deeper depths do not have organic matter remnants. These macropores are surrounded by a tightly packed clayey matrix with massive structure. Thin section analysis of a similarly structured acid sulfate soil from Indonesia by Bronswijk et al. (1993) showed that the acid sulfate soil immediately adjacent to macropores have experienced pyrite oxidation, whereas the pyrite contained in the soil matrix farther away from the structural features of the soil had not been oxidized. This has also been observed during profile description in Australia (Wilson 1999; Blunden and Indraratna 2000). The nature of the soil applied in this pyrite oxidation model is shown in Fig. 1 (a and b).

The schematic representation of the soil structure shows that oxygen diffuses vertically from the atmosphere into the soil through the air-filled macropores. The oxygen in the macro-

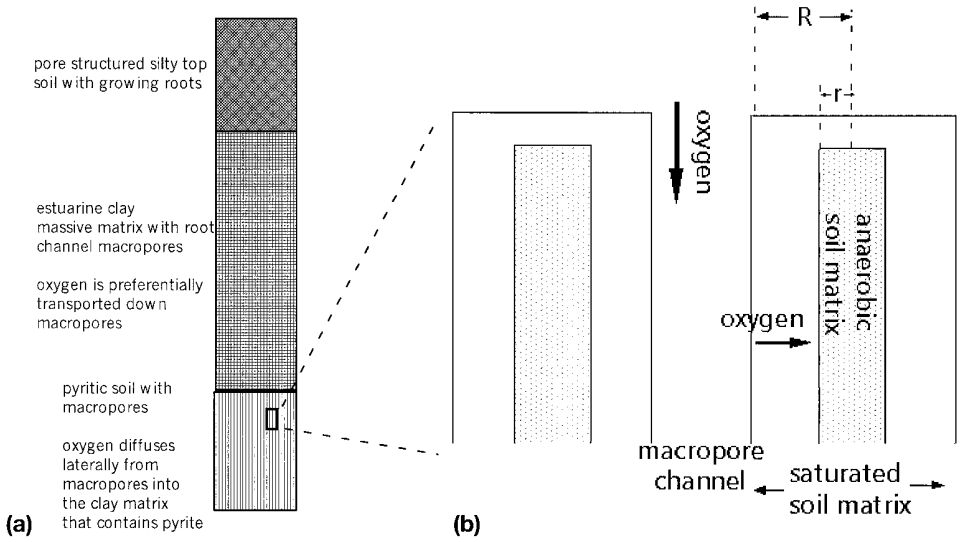

FIG. 1. Schematic of Soil Structure and Oxygen Transport in Pyrite Oxidation Model: (a) Soil Profile; (b) Oxygen Transport Down Macropores and into Pyritic Clay Matrix

pores is dissolved into the soil solution at the macropore walls where it can diffuse into the soil matrix. The dissolved oxygen is then consumed by pyrite oxidation. As shown in Fig. 1(b), a substantial part of the soil matrix between macropores is likely to remain in a saturated, anaerobic state due to capillarity and the moisture retention characteristics of the clayey matrix. However, as the ground-water table falls the macropores drain rapidly, thereby providing air-filled conjugates through which oxygen can quickly diffuse from the surface. As such, the transport of oxygen in the vertical orientation is controlled by the macropores and occurs at a rapid rate relative to the diffusion of oxygen through the clay matrix.

Similarly, the soil macroporosity plays a significant role in the lowering of the ground-water table. Blunden and Indraratna (2000) and Wilson et al. (1999) showed that the ground-water table can fall below the water level in nearby drains during periods of extended drought conditions. Given that active plant roots do not penetrate greater than approximately 0.5 m depth, reduction of the ground-water table elevation has been attributed to evaporation through these soil macropores.

The clayey nature of these estuarine sediments and their macropore-dominated structure control the transport of both air and water in the vertical and horizontal plane. Indraratna and Blunden (1999) showed that the saturated hydraulic conductivity (K_{sat}) in the vertical orientation was substantially greater than K_{sat} in the horizontal plane, particularly in the clayey soil horizons. The analysis of oxygen transport and subsequent pyrite oxidation described in this paper is limited to structured soil where air and water transport is dominant in the vertical orientation. The analysis may not be applicable for granular or well-packed materials such as sands, gravels, or for granular pyritic rock wastes.

Pyrite Oxidation in Aerobic Soil Matrix

The oxidation of pyrite is simulated in this model as the consumption of oxygen within the soil matrix. The amount of oxygen consumed during pyrite oxidation is dependent on the local oxygen concentration in the soil solution (Dent 1986). Bronswijk et al. (1993) showed that the relative importance of oxygen consumption by organic matter is very small in comparison to the oxygen consumed by pyrite. Therefore, the consumption of oxygen by organic matter is not explicitly modeled, but is assumed to be a constant small value where aerated conditions exist.

The oxidation of pyrite is based on the ''spherical reduction'' concept first described by Davis and Ritchie (1986) and subsequently adopted by most process-based numerical models of pyrite oxidation. This concept has two assumptions:

1. The rate of mass loss from the pyrite crystals as a result of oxidation is proportional to the surface area of the crystals.
2. The crystals are spheres of equal diameter.

The first assumption has been confirmed by Moses and Herman (1991) who showed that pyrite oxidation is a first-order rate reaction with respect to the surface/volume ratio of pyrite crystals. The second assumption is not valid for the distribution of pyrite in acid sulfate soils. However, the addition of a stochastic numerical scheme adds little with respect to the assessment of various acid sulfate soil management practices in a 3D landscape because the distribution of pyrite crystal size should be similar across a field site (Bush and Sullivan 1999).

Given these assumptions, the rate of pyrite dissolution by the consumption of oxygen is given by

$$\frac{\partial m}{\partial t} = -KA \tag{3}$$

where A = surface area of pyrite crystals (m^2); K = rate constant ($kg \cdot m^{-2}$ day^{-1}); m = the mass of pyrite (kg); and t = time (days).

In a unit volume (m^3) of acid sulfate soil

$$A = N\pi d^2 \tag{4}$$

where N = number of pyrite crystals/m^3 of acid sulfate soil; and d = diameter of the pyrite crystals (m).

The volume of pyrite in 1 m^3 of soil is equal to C_{FeS_2}/ρ, where C_{FeS_2} is the pyrite content ($kg \cdot m^{-3}$), and ρ is the density of pyrite ($kg \cdot m^{-3}$). The magnitude of N is then represented by

$$N = \frac{C_{FeS_2}/\rho}{\frac{1}{6}\pi d^3} \tag{5}$$

Substituting (5) into (4), the resulting expression from (3) gives

$$\frac{\partial m}{\partial t} = -K\frac{6C_{FeS_2}}{\rho d} \tag{6}$$

Eq. (6) shows that the rate of pyrite oxidation is dependent on a few easily determined parameters, i.e., C_{FeS_2} using wet chemical methods, d from thin section SEM, and ρ from literature. Obtaining an appropriate value of the rate constant K without resorting to site-specific empirical testing is more problematic. In the past, no rate constants have been evaluated specifically for pyrite oxidation in acid sulfate soil; however, a host of K values have been reported in the geochemical literature. These rate constants are usually derived from tightly controlled laboratory experiments using mixtures of pyrite crystals and water. It is not clear whether the laboratory-derived K values are applicable for the simulation of pyrite oxidation in the field.

McKibben and Barnes (1986) experimentally derived K values in the laboratory for similar temperature and pH conditions found in acid sulfate soils. McKibben and Barnes (1986) found that

$$K = 0.052\sqrt{C_w} \tag{7}$$

where C_w = concentration of dissolved oxygen (kg m^{-3}) in water.

In acid sulfate soil, C_w can be partitioned such that $C_w = C_p + C_{om}$, where C_p and C_{om} are the concentrations of oxygen consumed by pyrite and other factors such as organic matter decomposition, respectively.

Substitution of (7) into (6) gives

$$\frac{\partial m}{\partial t} = \frac{0.312C_{FeS_2}}{\rho d}\sqrt{C_p} + C_{om}\frac{0.312C_{FeS_2}}{2\sqrt{C_p}\rho d} \tag{8}$$

where $\partial m/\partial t$ now represents the rate of disappearance of pyrite crystals as a result of oxidation by oxygen and by the oxidation of organic substances in the soil. The consumption of oxygen by organic matter [i.e., the right-hand term in (8)] is small relative to the consumption of oxygen by pyrite oxidation (Bronswijk et al. 1993; White et al. 1997). It is therefore reasonable to either neglect the right-hand site of (8) or replace it with a small constant value OM. The organic matter concentration measured in the pyritic soil at the field site was <3% (Blunden and Indraratna 2000). Sensitivity analyses were conducted to determine the impact of C_{om} on $\partial m/\partial t$. The amount of oxygen consumed by 3% C_{om} when no pyrite was present in the soil was 14 kg/day. In comparison, the amount of pyrite consumed when both C_p and C_{om} are 3% was 2,907 kg/day. This indicated that the contribution of organic matter to overall oxygen consumption in the pyritic soil was very small. White

et al. (1997) suggested that the concentration of organic matter in Australian acid sulfate soils is very small and insufficient to promote the microbial reaction to reduce dissolved sulfate back to sulfide. Given the low concentration of organic matter in the soil, microbial activity involved in the decomposition of organic matter will have a small effect of both the pH and eH of the soil. However, at low pH, iron-reducing bacteria such as *Thiobacillus ferrooxidans* can act as a catalyst for the pyrite oxidation process (Dent 1986).

The stoichiometric reaction equation for pyrite oxidation by oxygen is (Bronswijk et al. 1993)

$$FeS_2 + \frac{15}{4} O_2 + \frac{1}{2} H_2O \rightarrow Fe^{3+} + 2SO_4^{2-} + H^+ \quad (9)$$

Therefore, under aerobic conditions, 1 mol of pyrite consumes 3.75 mol of oxygen, which is equal to 1 kg of pyrite consuming 1 kg of oxygen during complete oxidation. Thus, (8) may also be expressed as the mass oxygen consumption rate α_m by pyrite oxidation within the soil matrix, that is

$$\alpha_m = \frac{0.311 C_{FeS_2}}{\rho d} \sqrt{C_p} + OM \quad (10)$$

Oxygen Transport in Soil Matrix

At some distance [$R - r$ (R = radius of the soil aggregates and r = radius of the anaerobic zone); Fig. 1] from the macropore wall into the soil matrix, the consumption of oxygen by pyrite will equal the supply of oxygen through the macropore wall. The remainder of the soil matrix is assumed to remain anaerobic. This is due to the low oxygen diffusion coefficients for the wet clayey soil matrix and the high rate of oxygen consumption in the aerobic zone immediately adjacent to the macropore as a result of pyrite oxidation. In the aerobic part of the soil matrix, the oxygen concentration decreases from the macropore wall to zero at the aerobic-anaerobic boundary.

A differential equation describing the oxygen diffusion and consumption in the soil matrix away from the macropore wall needs to be solved in order to calculate the dissolved oxygen concentration profile and aerobic volume in the matrix. The formulation of such a differential equation and its solution depend on the geometry of the soil structure. Nevertheless, where the length of the oxygen diffusion path is small and the consumption of oxygen by pyrite is high, the diffusion of dissolved oxygen can be approximated by diffusion into a semi-infinite block. On the basis of this assumption, the steady-state diffusion equation for the aerobic part of the soil matrix [(2)], where the oxygen consumption term is described by (10), can be written as

$$D_w \frac{d^2 C_w(x)}{dx^2} = \frac{0.311 C_{FeS_2}}{\rho d} \sqrt{C_p} + OM \quad (11)$$

where D_w = diffusion coefficient of oxygen in the soil aggregate ($m^2\ day^{-1}$). The boundary conditions for (11) per Fig. 1(b) are

$$\text{at } x = r \quad dC_w(x)/dx = 0$$

$$\text{at } x = R \quad C_w(x) = C_b$$

C_b is the concentration of oxygen in the water at the boundary between the soil matrix and the macropores ($kg \cdot m^{-3}$), and is calculated according to Henry's law

$$[O_2]_{air} = H_k \times [O_2]_{water} \quad (12)$$

where H_k = temperature dependent Henry's constant; and $[O_2]_{air}$ and $[O_2]_{water}$ = concentrations of oxygen in air and water, respectively.

Given that changes in the pyrite concentration and the diameter of pyrite crystals are very small for small time steps (say, hourly), the values for C_{FeS_2} and d in (11) can be held constant for one model time step (1 day).

In order to speed up the solution convergence, a linear relation between oxygen consumption and dissolved oxygen concentration was determined. Using such a linear approximation, the right-hand side of (11) becomes

$$D_w \frac{d^2 C_w(x)}{dx^2} A' C_p(x) + OM' \quad (13)$$

where $A'C_p(x)$ = apparent mass oxygen consumption rate resulting from pyrite oxidation, where A' is a constant and OM' is the intercept on the axis of the oxygen consumption rate, where the oxygen consumption by pyrite is zero. OM' may be considered as the apparent mass oxygen consumption rate resulting from other oxygen-consuming processes, e.g., organic matter or bacteria.

Solving (13) gives an expression (14) for the steady-state oxygen concentration in the aerobic part of the soil matrix, i.e., $r < x < R$

$$C_p(x) = \left(C_b + \frac{OM'}{A'}\right)\left\{\frac{\cosh\sqrt{\beta}(x - r)}{\cosh\sqrt{\beta}(R - r)}\right\} - \frac{OM'}{A'} \quad (14)$$

Hence, the radius of the anaerobic zone is

$$r = R - \frac{\cosh^{-1}\chi}{\sqrt{\beta}} \quad (15)$$

where $\beta = A'/D_w$; and $\chi = 1 + A'C_b/OM'$. For the anaerobic part of the soil matrix ($x < r$), $C_w(x) = 0$.

By calculating the radius of the anaerobic zone $r(m)$ and solving (14) for $C_p(x)$ for $r < x < R$, the total mass of oxygen consumed φ_T ($kg \cdot m^{-3}\ day^{-1}$) in the soil matrix can be determined by

$$\varphi_T = \int_r^R [A'C_p(x) + OM']\, dx \quad (16)$$

The solution to (16) becomes

$$\varphi_T = \left[\frac{A'C_b + OM'}{\sqrt{\beta}}\right] \tanh\sqrt{\beta}(R - r) \quad (17)$$

S_o is now defined as the specific surface area of the soil through which oxygen diffusion takes place in 1 m^3 of soil or a measure of the soil structure. In this model, the soil structure within the matrix is assumed to be a plate structure, hence, $S_o = 1/R$. Thus, (17) becomes

$$\varphi_T = \left(\left[\frac{A'C_b + OM'}{\sqrt{\beta}}\right] \tanh\sqrt{\beta}(R - r)\right) \times S_o \quad (18)$$

The calculation of the amount of oxygen consumption by organic mater (φ_{OM}) is simple because it is assumed to be at a constant rate in the aerobic fraction of the soil matrix $(R - r)/R$, whereby

$$\varphi_{OM} = \frac{OM'(R - r)}{R} \quad (19)$$

Thus, the steady-state amount of oxygen consumed by pyrite oxidation is calculated by

$$\varphi_{FeS_2} = \varphi_T - \varphi_{OM} \quad (20)$$

From the amount of oxygen consumed by pyrite [(20)], the amount of pyrite oxidized is calculated, and the production of Fe^{2+}, H^+, and SO_4^{2-} is determined accordingly.

Oxygen Diffusion and Consumption in Macropores

The vertical, steady-state oxygen distribution in the air-filled macropores is described by (2). The consumption term (α_v) is derived from the mass consumption of oxygen at the macropore walls (φ_T). Application of the Boyle-Gay-Lussac law gives

$$D_s(n_e)\,\frac{\partial C_a(x)}{\partial x^2} = \alpha_v = 2.56 \times 10^{-3} \cdot T \cdot \varphi_T \tag{21}$$

where T = absolute temperature (K).

Numerous empirically derived analytical equations describing a relationship between the air-filled porosity and the oxygen diffusion coefficient exist in the literature. In this model, the oxygen diffusion through the macropores is described by (Troeh et al. 1982)

$$D_s(\varepsilon) = \left(\frac{\varepsilon - 0.01}{0.99}\right)^{1.3} \times D_o \tag{22}$$

The transport of oxygen down macropores and through the soil matrix in conjunction with simultaneous consumption of oxygen by pyrite oxidation is the key to this model. The oxygen concentration in the air-filled macropores is dependent on the consumption of oxygen at the macropore walls. Simultaneously, the oxygen consumption inside the clay matrix is dependent on the oxygen concentration in the air-filled macropores. These calculations are solved by an iterative process in the numerical model.

PYRITE OXIDATION NUMERICAL MODEL

The pyrite oxidation model (ACID3D) was developed to work in conjunction with the output from FEMWATER, a

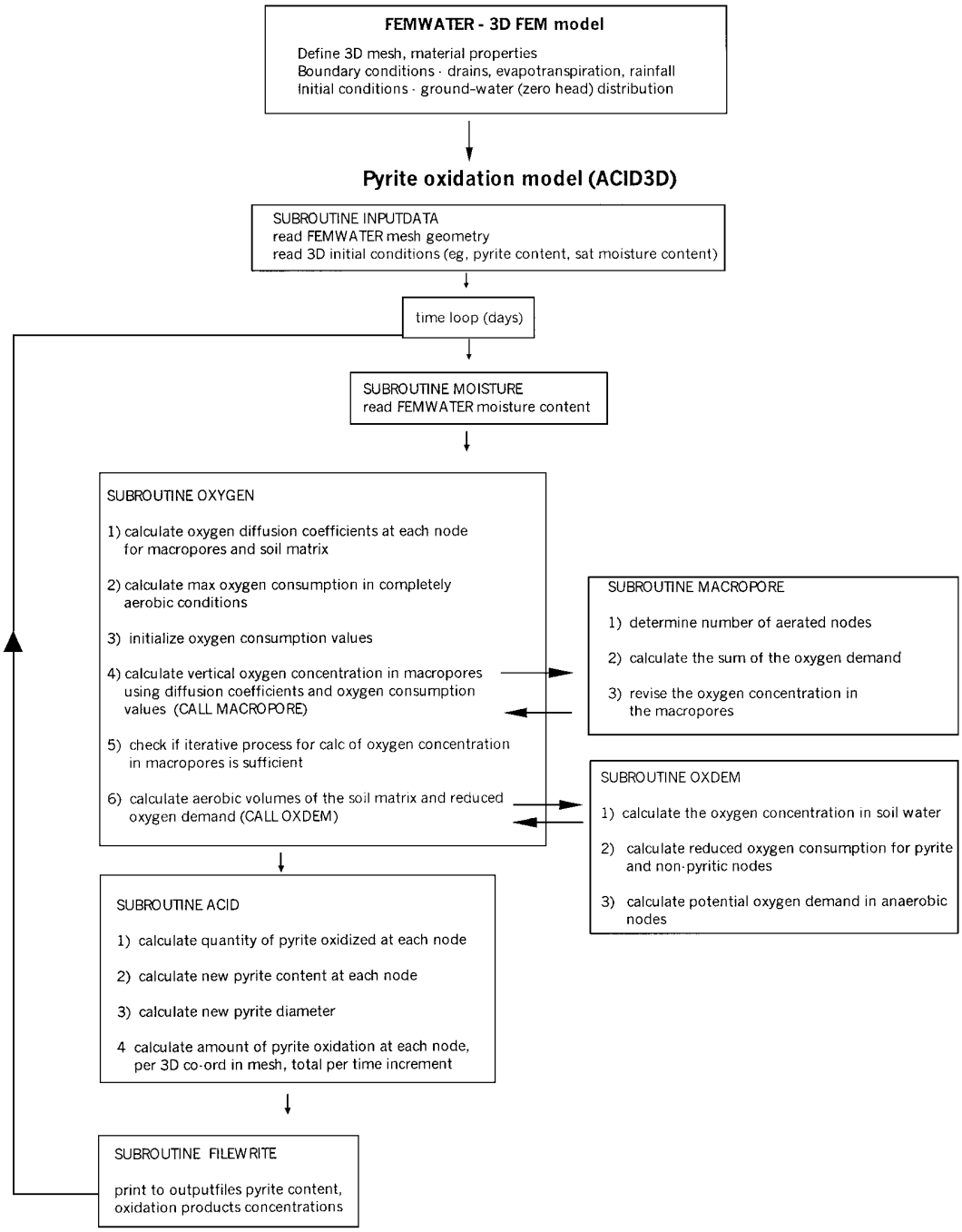

FIG. 2. Flowchart of FEMWATER and ACID3D Models

commercially available saturated-unsaturated ground-water flow model (Lin et al. 1997). A flowchart of the FEMWATER-ACID3D model process is shown in Fig. 2.

COMPARISONS BETWEEN ANALYTICAL AND NUMERICAL SOLUTIONS

A comparison was made between the numerical solution of (11) and the analytical solution of the linear approximation [i.e., (18)], to determine the oxygen consumption due to pyrite oxidation for pyrite concentrations of A (52.2 $kg \cdot m^{-3}$) and B (15.2 $kg \cdot m^{-3}$), which represent the typical range of highest and lowest pyrite concentrations found in pyritic soils in Southeastern Australia (White et al. 1997). A summary of the analytical and numerical factors used in the model are shown in Table 1.

Fig. 3 shows that there is good agreement for the calculation of oxygen consumption depending on the local dissolved oxygen concentration according to (11) and its linear approximation, (13), for high and low pyrite concentrations. The solutions were calculated for $0 < C_p < 0.005$, which is the likely range for dissolved oxygen concentrations for the climatic conditions prevalent in temperate and subtropical Australia (White et al. 1997).

Fig. 4 shows excellent agreement between the dissolved oxygen concentration profiles extending from the macropore wall into the soil matrix obtained with the analytical solution [(13)] and the numerical solution of (11). The most important parameter in the comparison of the numerical and analytical solutions is the value of the mass of oxygen consumption in the soil matrix (φ_T). The value of φ_T determines the amount of pyrite oxidized in the soil matrix [(18)]. The difference between the analytical and numerical solutions was very small. Values of φ_T for the two pyrite concentrations described above are shown in Table 2. The small difference between the numerical and analytical solutions indicates that the model accurately simulated the oxidation of pyrite in the soil matrix given the various assumptions implicit in the model.

TABLE 1. Factors of Analytical and Numerical Solutions for Two Pyrite Concentrations

Variable (1)	A (2)	B (3)
C_{FeS_2}	52.2	15.2
A	64.98	18.89
OM	0.08	0.08
A'	627.71	182.53
OM'	1.43	0.42
C_b	5.17×10^{-3}	4.93×10^{-3}
R	6.67×10^{-3}	6.67×10^{-3}
r	6.43×10^{-3}	6.24×10^{-3}

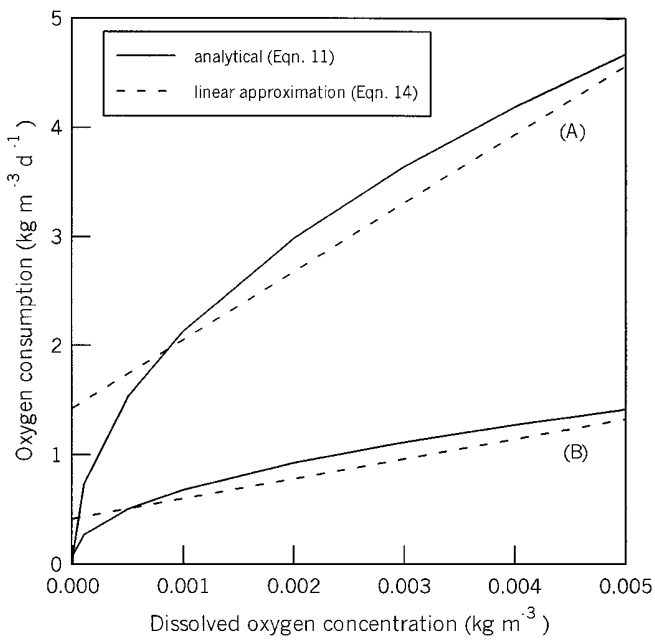

FIG. 3. Solution of Eqs. (11) and (14) for Oxygen Consumption as Function of Dissolved Oxygen Concentration

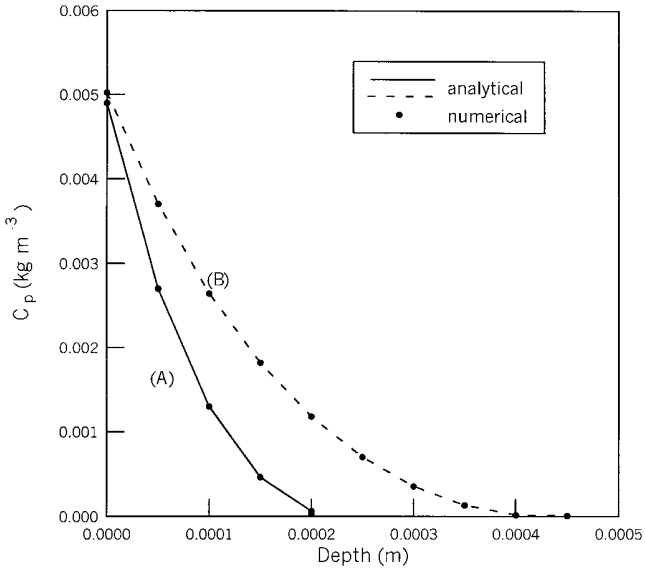

FIG. 4. Dissolved Oxygen Concentration Profiles Extending from Macropore Channel into Saturated Soil Matrix

TABLE 2. Analytical and Numerical Values for φ_T

Pyrite concentrations ($kg \cdot m^{-3}$) (1)	Numerical φ_T (2)	Analytical φ_T (3)	Percent difference (4)
A	0.085	0.084	1.1
B	0.047	0.044	2.2

CASE STUDY: ASSESSMENT OF PYRITE OXIDATION FOR TWO DRAINAGE REGIMES

Simulations using ACID3D were carried out using soil and ground-water hydrology data collected from a field study site where an acid sulfate soil-ground-water management trial is currently under way. The study site is a small subcatchment of approximately 120 ha that has been drained for agricultural and flood mitigation purposes. The site is adjacent to the township of Berry on the south coast of New South Wales, Australia. A network of deep flood mitigation drains was constructed across the site in the late 1960s. The drains discharge into Broughton Creek, a left-bank tributary of the Shoalhaven River through one-way floodgates that discharge during low tide. The site is typical of coastal floodplains in New South Wales with a maximum elevation of 4 m relative to the Australian Height Datum (AHD) and the lowest elevation <1 m AHD. Sulfidic sediments were formed during the Holocene period under a barrier estuary environment (Roy 1984) and have subsequently been covered with shallow layers of varying thickness.

The deep flood mitigation drains have caused the water table to be lowered below the acid sulfate soil layer due to ground-water drawdown. Low ground-water tables cause acid generation when the pyritic soil is exposed to oxidizing conditions.

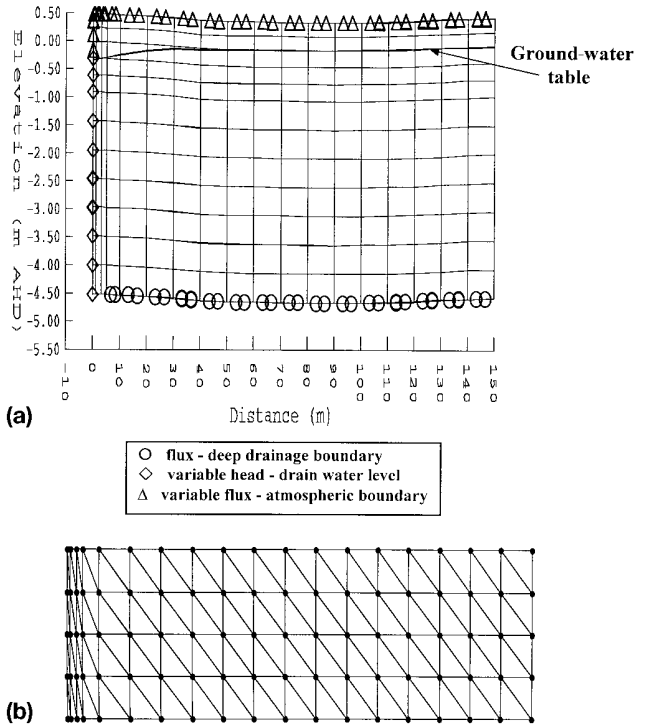

FIG. 5. Schematic of FEMWATER Mesh: (a) Side Elevation View Showing Boundary Conditions and Initial Ground-Water Level; (b) Plan View Showing Triangular Element Geometry and Nodes

Temporary weirs have been installed in the flood mitigation drains to raise drain water levels above the pyritic soil layer in order to minimize ground-water drawdown and reduce the rate of acid discharge into the drains.

The natural drain water response and an alternative weir management strategy were simulated using FEMWATER by constructing a finite-element mesh 150 m long, 5 m deep, and 40 m wide. The complete mesh consisted of 1,235 elements and 1,728 nodes. Material properties that were determined from intact samples collected from the study site were assigned to six soil layers. The atmospheric and drain water-level boundaries were determined from field data collected during 1997 and 1998. The FEMWATER mesh with symbols showing various boundary conditions and the initial ground-water elevation is shown in Fig. 5(a). The plan view of the mesh showing the element geometry and location of the nodes is shown in Fig. 5(b). A comprehensive description of the study site and the soil physical properties can be found in Blunden and Indraratna (2000). The atmospheric boundary was defined as a transient variable flux at the nodes at the top of the finite-element mesh. The drain water levels were defined as either a variable head (i.e., drain simulation) or as a constant head (i.e., weir simulation) at the elements across the drain-soil interface. Losses of ground water via deep drainage were defined by a variable flux boundary at the nodes on the bottom of the mesh. The initial static water pressure was taken from piezometer data collected at the site and applied as a pressure head distribution for the saturated and unsaturated parts of the soil profile. FEMWATER used a pointwise iterative matrix solver in conjunction with a Gaussian quadrature scheme. A maximum of 40 iterations were allowed for solving the non-linear flow equation, or until a steady-state convergence criterion of 10^{-3} was achieved.

Observed and Simulated Ground-Water Profiles

Two ground-water regimes were simulated using FEMWATER. The first simulation used the drain water levels measured at the field site as input for the variable head boundary used to model the drain water level. This is referred to as the "drain simulation," which represents the water level in the flood mitigation drains as determined by the operation of the floodgate [Fig. 6(a)]. The second simulation involved maintaining a constant head boundary to represent a drain water elevation of −0.5 m AHD [Fig. 6(b)]. This is referred to as the "weir simulation," which represents the situation where the water level in the drains is maintained at a predetermined constant level by the installation of weirs. A substantial increase in the simulated elevation of the ground-water table was achieved by maintaining the water level of the drain at −0.5 m AHD. The ground-water elevations at 10 and 90 m distance from the drain for the two simulations, as well as the observed piezometer data for the drained state, are shown in Fig. 7. The model predictions for the drained simulation are in good agreement with the observed piezometer data.

Simulated Pyrite Oxidation

The ground-water profiles for the drain and weir simulations were used as inputs for the ACID3D model. The upper boundary of the pyritic layer was at a depth of −0.65 m AHD and extended to a depth of −2 m AHD. The pyrite concentration was less than 3% (Table 3). The initial diameter of pyrite crystals was 1 μm. The magnitude and distribution of sulfate production caused by pyrite oxidation in the pyritic soil during the simulation for the two ground-water management strategies is shown in Fig. 8, for three different periods.

Fig. 8 shows that the extent of pyrite oxidation across the study area varies with time, and is dependent on the elevation of the ground-water table. At Day 170, the ground-water table had fallen below the acid sulfate soil layer. The zone of pyrite oxidation extends across the whole simulation area for the drained situation and has progressed down approximately 0.6 m into the pyritic layer. The pyrite oxidation zone in the weir simulation is not as extensive in either areal extent or depth at Day 170.

The ground-water table fell to its maximum depth around Day 220. In the drain simulation, pyrite oxidation extended in excess of 1 m into the acid sulfate soil layer, whereas pyrite oxidation occurred in the upper 0.6 m of the pyritic layer for the weir simulation. The thickness of the oxidized zone is substantially less close to the drain than further out into the field. For both the drain and weir simulations, the ground-water table is supplemented by seepage through the drain walls for the area immediately adjacent to the drain. At distances >20 m from the drain, evaporative losses from the ground water are greater than the recharge rate, thereby giving rise to lower ground-water table elevations away from the drain. This in turn enables the pyrite oxidation front to progress to deeper depths as the distance increases away from the drain.

By Day 310 the ground-water table had risen as a result of significant rainfall. The ground-water table was higher than the acid sulfate soil layer across the whole site for the weir simulation which precluded further pyrite oxidation. In contrast, a small area of pyrite oxidation still occurred for the drain simulation. Though the volume of oxidizing acid sulfate soil appears relatively small to that previously exposed to oxidizing conditions, the ongoing oxidation of pyrite in the acid sulfate soil layer immediately adjacent to the drains still poses a severe problem for the water quality in the drain. As acidic pyrite oxidation products are generated in this volume of soil close to the drain, small rainfall events will ensure that acid is continually discharged into the drainage system.

Simulation of the ground-water regime and oxidation of pyrite in acid sulfate soil layers using the 3D modeling approach described above allows for direct comparison of the effectiveness of various management options at a field or subcatchment

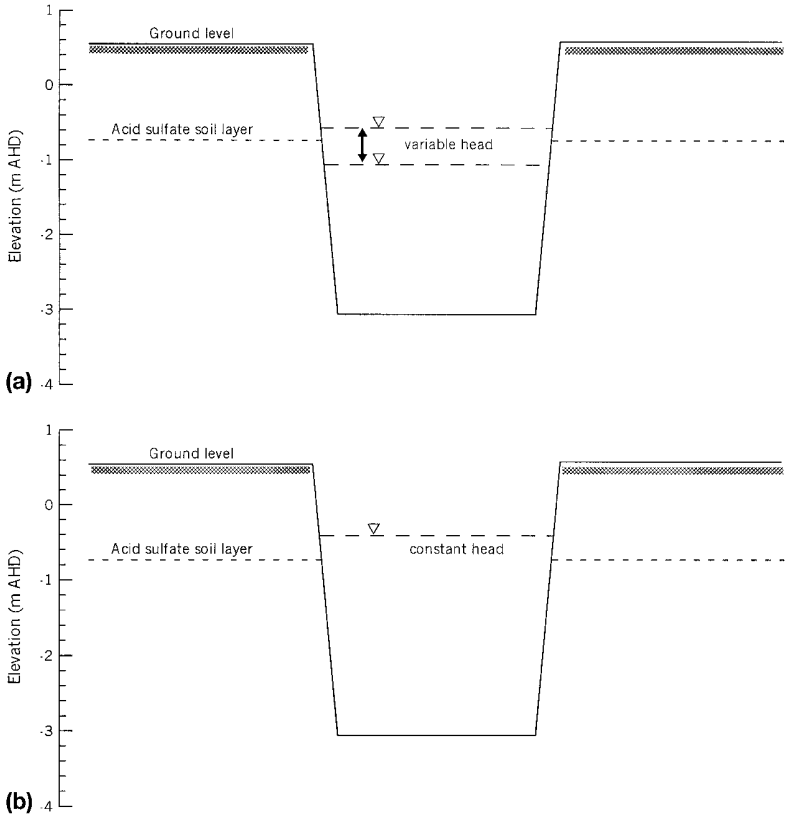

FIG. 6. Simulated Head Boundaries for Drain Water Levels: (a) Drain Simulation Using Variable Head; (b) Weir Simulation Using Constant Head

scale. Fig. 9 shows the amount of sulfate generated during the simulation period for the drain and weir alternatives.

The onset of pyrite oxidation was delayed in the weir simulation relative to the drained situation. In periods where drought conditions may not have been as severe as those experienced during this period, pyrite oxidation may be avoided by maintenance of higher ground-water levels as a result of the weir. The amount of pyrite oxidation was also lower for the weir simulation as a smaller volume of pyritic soil was exposed to oxidizing conditions at any specific day.

The amount of sulfate produced by pyrite oxidation was 91×10^3 for the drain simulation, whereas the weir alternative only produced 43×10^3 mol of sulfate. This represents a 53% reduction in the generation of acidic pyrite oxidation products as a result of applying a higher water level in the drain using a weir. These predictions suggest that maintenance of higher water levels within the drains by installing weirs will have substantial benefits in reducing the amount of acid produced during pyrite oxidation.

Comparison of ACID3D Predictions with Field Data

The pyrite concentration of the sulfidic soil at elevations of -0.7, -1.0, and -1.5 m AHD was determined from samples collected at 90 m distance from the drain at the end of the simulation period. The measured pyrite concentrations at these depths at both the start and end of the simulation period, as well as the predictions made by ACID3D at the end of the simulation, are shown in Table 3.

The computed pyrite concentration in the soil profile after 365 days for the drain simulation correspond well with the measured pyrite concentration from the field. The amount of pyrite consumed during oxidation was slightly underestimated (by 0.09%) at the -0.7 m AHD depth node relative to the pyrite concentration measured on field samples. At -1.0 m AHD, a very small overestimate of the amount of pyrite oxidized was calculated by ACID3D. Given the likely variability in the pyrite concentration of the sulfidic soil, the calculation of pyrite concentration by ACID3D is in good agreement with field data.

The cumulative amount of sulfate produced by pyrite oxidation was 91×10^3 mol for the drain simulation. This compares well with the theoretical amount of sulfate generated by pyrite oxidation in the field. Calculation of the amount of sulfate produced by pyrite oxidation from the difference between the initial and final pyrite concentrations (Table 3) shows that approximately 127×10^3 mol of sulfate was generated in the field. The underestimation of the amount of sulfate generated from the oxidation of pyrite by ACID3D may stem from a number of factors. First, the distribution of pyrite oxidation is not even across the study area, with less pyrite being oxidized close to the drain. Hence, the approximation of 127×10^3 mol of sulfate being generated from the theoretical calculation based on initial and final pyrite concentrations at 90 m distance from the drain may be an overestimate of the total amount of pyrite actually oxidized. Another important factor is the distribution of pyrite crystals within the soil structure/matrix. For computational simplicity, the ACID3D model, as well as many other pyrite oxidation models [e.g., Bronswijk et al. (1993) and Wunderly et al. (1996)], assume that pyrite is uniformly distributed throughout the soil matrix. However, Bush and Sullivan (1999) show that a considerable proportion of the pyrite occurs within and adjacent to macropores. This pyrite would be more prone to oxidation compared with pyrite distributed away from the macropores due to the preferential and rapid diffusion of oxygen down the macropores. The amount of sulfate generated by pyrite oxidation by ACID3D is approximately 72% of that determined by the difference between the initial and final pyrite concentration measured from the field. Dent (1986) suggested that many pyrite oxidation models un-

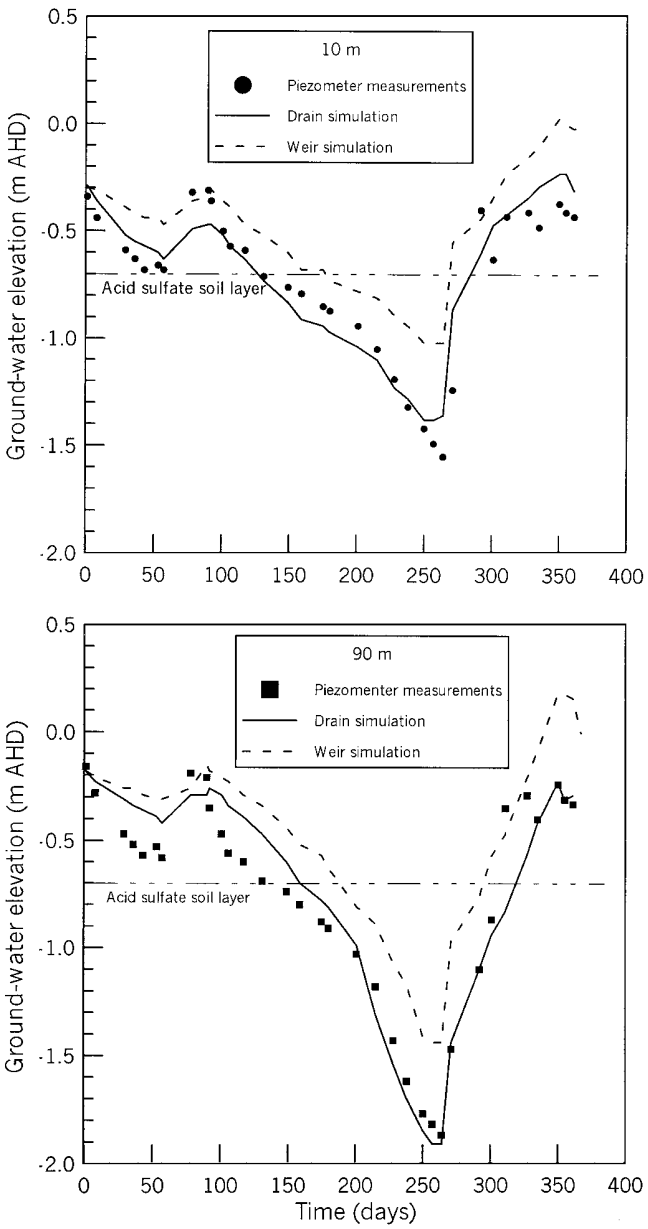

FIG. 7. Observed and Predicted Ground-Water Elevations at 10 and 90 m from Drain

TABLE 3. Measured and Simulated Pyrite Concentrations

Elevation (m AHD) (1)	Initial observed pyrite concentration (percent) (2)	Final simulated pyrite concentration (percent) (3)	Final observed pyrite concentration (percent) (4)
−0.7	2.26	2.06	1.97
−1.0	1.60	1.49	1.50
−1.5	0.20	0.20	0.20

derestimate the actual field oxidation rate by about 30%, and Bush and Sullivan (1999) argued that the distribution of pyrite and its relationship to soil structure may have been the reason for this underestimation.

The prediction of pyrite oxidation by ACID3D is further confirmed by soil and ground-water quality data measured at the start and end of the simulation period, respectively. These data are shown in Figs. 10 and 11. As shown in Fig. 10, the concentration of soluble sulfate in the soil within and immediately above the pyritic layer increased substantially over the study period. This increase is attributed to pyrite oxidation that occurred during the period where the ground-water table fell into the pyritic soil. The generation of pyrite oxidation products is also confirmed by the reduction of the soil pH in and above the pyritic soil layer, and the increase in electrical conductivity associated with the increased concentration of dissolved sulfate, iron, and aluminum in the soil.

The concentration of dissolved sulfate in ground water measured at 10 and 90 m distance from the drains also confirms the magnitude and distribution of pyrite oxidation caused by the low ground-water table. As shown in Fig. 11, the concentration of sulfate in the ground water remains relatively stable until Day 270, when sulfate generated by pyrite oxidation between days 170 and 260 was entrained into the rising ground-water table. The concentration of sulfate in the ground water after Day 270 reflects the distribution of pyrite oxidation away from the drain. Fig. 8 shows that the simulated sulfate production extends to a great depth at 90 m distance from the drain, relative to the depth of sulfate production at 10 m distance from the drain. The substantial increase in the magnitude of the concentration of sulfate in the ground water at 90 m in comparison to 10 m confirms the distribution of simulated pyrite oxidation using ACID3D.

Given the assumptions within the ACID3D model and field variability, the simulated and measured data are in close agreement, and they demonstrate that ACID3D accurately calculates the amount of pyrite oxidized. The exact magnitude of the amount of pyrite oxidized, and the corresponding amounts of acidic oxidation products generated, can be considered of secondary importance, particularly where the objective of the ACID3D model is to determine the relative merits of potential drain management schemes that may reduce the generation of acidic pyrite oxidation products. Ground-water drawdown or recharge by seepage from the drain into the soil is not uniform across the study site. As such, the study of drain management alternatives relative to their influence on the soil moisture content distribution across a site and hence the amount of pyrite oxidized under any particular drain management scheme can be successfully investigated using the FEMWATER-ACID3D modeling system.

OTHER MECHANISMS OF PYRITE OXIDATION

The numerical modeling phase of this study is focused on the primary mechanism of pyrite oxidation [(9)], whereby 1 kg of pyrite consumes approximately 1 kg of oxygen to produce 1.5 kg of acid during the complete reaction. In this case study, as the organic content in and close to the pyritic clay layer is very small (<2%), the role of biotic oxidation is not expected to be significant, hence, not modeled within the scope of this study. Nevertheless, it is of relevance to note that under favorable conditions of pH < 3, high temperature and relatively high organic content (say, 5%), microbial catalytic pyrite oxidation rates can be much higher than abiotic pyrite oxidation rates (Dent 1986; Chapman and Murphy 2000). In pyritic clays from Southeast Asia, Bronswijk et al. (1993) found that sterilized samples had the same rate of pyrite oxidation as unsterilized samples. This indicates that the mechanisms that facilitate biotic pyrite oxidation may not be significant in all pyritic media.

Where pH is <3, Fe^{3+} [(9)] can directly oxidize pyrite, while it is still undergoing primary oxidation

$$FeS_2 + 14Fe^{3+} + 8H_2O \rightarrow 15Fe^{2+} + 2SO_4^{2-} + 16H^+ \quad (23)$$

However, sulfate production via the above reaction is secondary, i.e., 14 mol of ferric ions to produce 2 mol of sulfate ions, in comparison with the primary oxidation reaction of pyrite represented in (9). As such, if both the primary and secondary

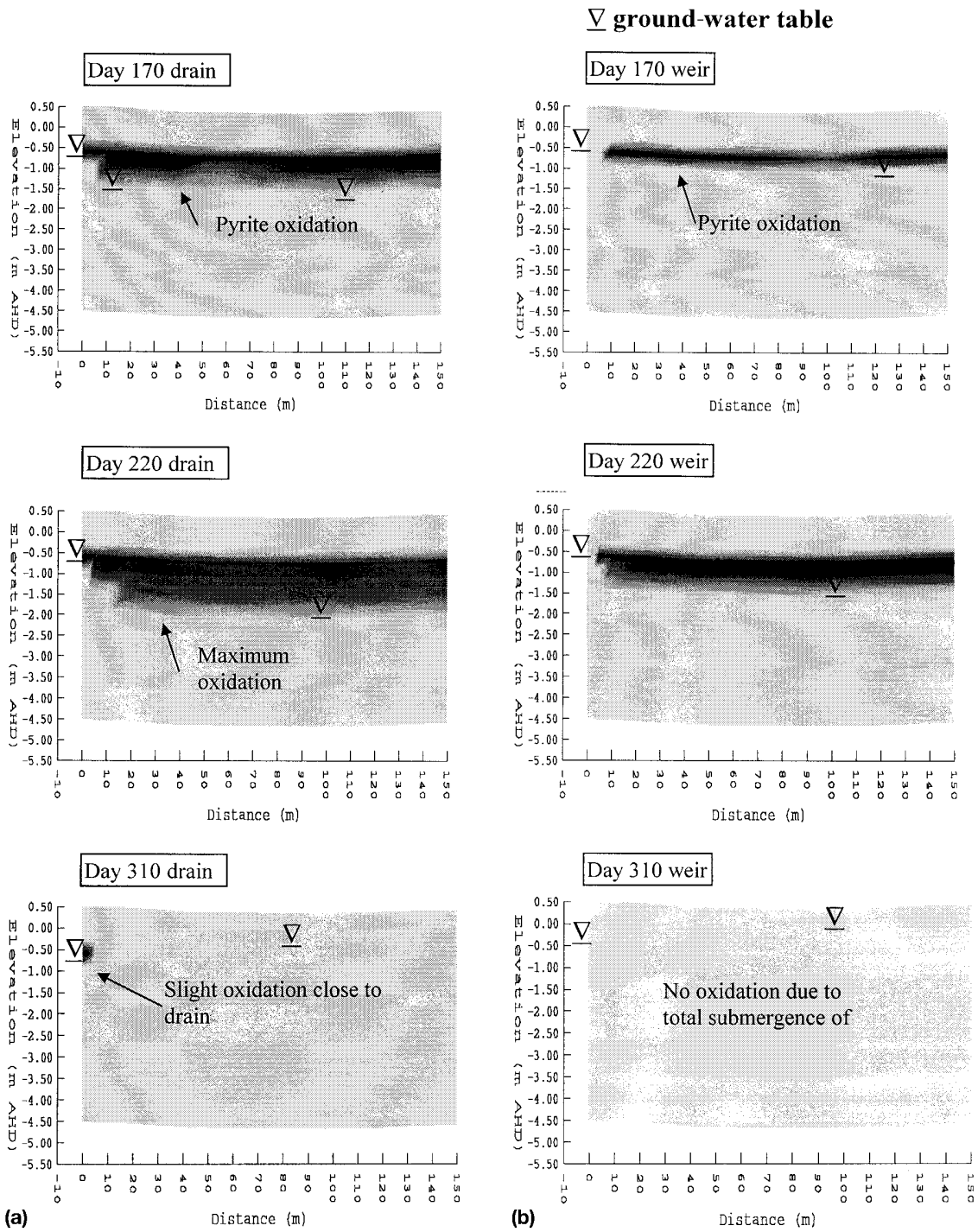

FIG. 8. Simulated SO_4 Production from Pyrite Oxidation Using ACID3D for (a) Drain and (b) Weir Management Options

pyrite oxidation reactions were to occur simultaneously, only a small amount of sulfate concentration could be attributed to the abiotic oxidation reaction described by (23).

Finally, a fraction of the soluble Fe^{2+} may be exported to receiving waters of higher pH, where subsequent oxidation to ferric hydroxides or oxyhydroxides produces more acid at a considerable distance away from the original pyrite source

$$Fe^{2+} + \frac{1}{4} O_2 + \frac{7}{2} H_2O \rightarrow FeOOH + 2SO_4^{2-} + 4H^+ \quad (24)$$

As the above reaction contributes to ''acid at a distance'' (White et al. 1997), the authors have not modeled this process.

SUMMARY AND CONCLUSIONS

In the past, many pyrite oxidation models have simulated the uniform diffusion of oxygen through the pyritic material, where the oxygen then becomes available for pyrite oxidation. This is not valid for a structured acid sulfate soil with well-defined macropores. A new theoretical approach for simulating the transport of oxygen into a macropore-structured acid sulfate soil, and the subsequent diffusion of oxygen laterally into the soil matrix, has been described. As oxygen is transported into the soil matrix, the oxygen is consumed by pyrite oxidation and other oxygen-consuming processes. The amount of pyrite oxidation products is then calculated from the mass of

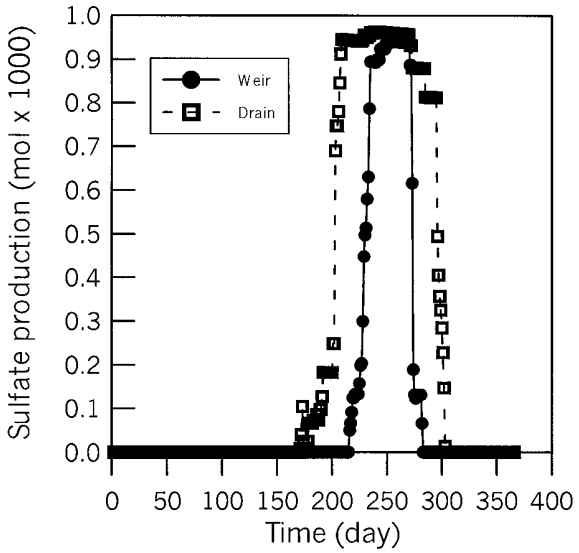

FIG. 9. Simulated Sulfate Production from Pyrite Oxidation for Drain and Weir Management Options

oxygen consumed by pyrite. Oxygen consumption by organic matter is small in comparison with pyrite oxidation.

A computer simulation model, ACID3D, was developed using a linear approximation of the equation for oxygen transport into the aerobic part of the soil matrix. The numerical linear approximation was in good agreement with the theoretical (analytical) solution for both the oxygen consumption by pyrite and organic matter with respect to the local oxygen concentration, and the transport of dissolved oxygen into the soil matrix. When combined with a commercially available unsaturated/saturated ground-water flow model, ACID3D was able to simulate the magnitude and distribution of pyrite oxidation in a 3D space. The magnitude and distribution of sulfate generated by pyrite oxidation was shown to be in general agreement with the soil and ground-water quality data measured in the field.

The application of ACID3D allows for the assessment of potential acid sulfate soil-management techniques that involve manipulation of the ground-water table. This was illustrated in the presentation of a case study where two drain management options were assessed. The simulation model predicted that a 53% reduction in the amount of pyrite oxidized could be

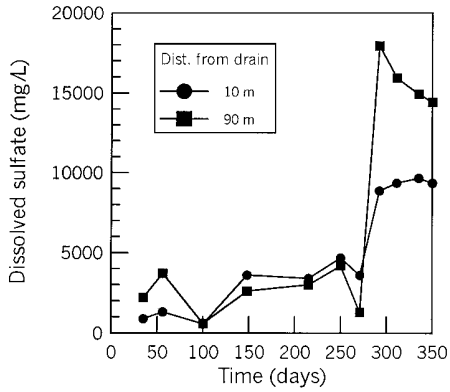

FIG. 11. Measured Dissolved Sulfate Concentration at 10 and 90 m Distance from Drain

achieved if the water level in the drain was maintained at −0.5 m AHD by the installation of a weir, as opposed to the lower drain water level that occurred under normal drain operating conditions. The case study showed that the magnitude and distribution of pyrite oxidation varies spatially and temporally, and that it is largely determined by the ground-water hydrology of the site.

ACKNOWLEDGMENTS

The Australian Research Council and New South Wales Government provided financial assistance for this research under the ARC-SPIRT and ASSPRO programs, respectively. Dr. Andrew Nethery (NSW EPA) and John Downey (Shoalhaven City Council, NSW) assisted with the development of the study site.

APPENDIX. REFERENCES

Blunden, B., and Indraratna, B. (2000). ''Evaluation of surface and ground-water management strategies for drained acid sulfate soil using numerical simulation models.'' *Australian J. of Soil Res.*, 38, 569–590.

Bronswijk, J., Nugroho, K., Aribawa, J., Groenberg, J., and Ritsema, C. (1993). ''Modeling of oxygen transport and pyrite oxidation in acid sulfate soils.'' *J. Envir. Quality*, 22(2), 544–554.

Bush, R., and Sullivan, L. (1999). ''Pyrite morphology in three Australian Holocene sediments.'' *Australian J. of Soil Res.*, 37, 637–653.

Chapman, P. E. V., and Murphy, B. W. (2000). *Soils—their properties and management*, 2nd Ed., Oxford University Press, New York.

Davis, G., and Ritchie, A. (1986). ''A model of oxidation in pyritic mine wastes: Part 1. Equations and approximate solution.'' *Appl. Math. Modelling*, 10(2), 314–322.

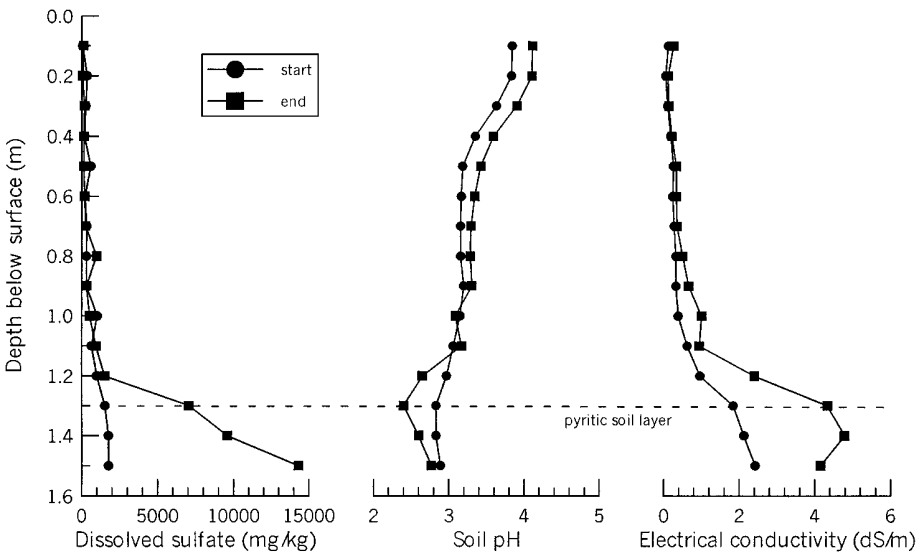

FIG. 10. Measured Soil Chemical Properties at Start and End of Simulation Period Showing Evidence of Pyrite Oxidation

Dent, D. (1986). ''Acid sulfate soils: A baseline for research and development.'' *Publ. No. 39*, Int. Inst. for Land Reclamation and Improvement, Wageningen, The Netherlands.

Elberling, B., Nichlson, R., and Scharer, J. (1994). ''A combined kenitic and diffusion model for pyrite oxidation in tailings: A change in controls with time.'' *J. Hydro.*, Amsterdam, 157(1), 47–60.

Hodgson, A., and MacLeod, D. (1989). ''Use of oxygen flux density to estimate critical air-filled porosity of a Vertisol.'' *Soil Sci. Soc. Am. J.*, 53(2), 335–361.

Indraratna, B., and Blunden, B. (1999). ''Nature and properties of acid sulphate soils in drained coastal lowlands in New South Wales.'' *Australian Geomechanics J.*, 34(1), 61–78.

Jaynes, D., Rogowski, A., and Pionke, H. (1984). ''Acid mine drainage from reclaimed coal strip mines 1. Model description.'' *Water Resour. Res.*, 20(2), 233–242.

Lin, H., et al. (1997). ''FEMWATER: A 3D finite-element computer model for simulating density-dependent flow and transport in variably saturated media.'' *Tech. Rep. CHL-97-12*, U.S. Army.

McKibben, M., and Barnes, H. (1986). ''Oxidation of pyrite in low temperature acidic solutions: Rate laws and surface textures.'' *Geochimica Cosmochimica Acta*, 50, 1509–1520.

Moses, C., and Herman, J. (1991). ''Oxidation of pyrite in low temperature acidic solutions: Rate laws and surface textures.'' *Geochimica Cosmochimica Acta*, 50, 1509–1520.

Nyguyen, T., and Wilander, A. (1995). ''Chemical conditions in acidic waters in the Plain of Reeds, Vietnam.'' *Water Res.*, 29, 1401–1408.

Refsgaard, J., Christensen, T., and Ammentorp, H. (1991). ''A model for oxygen transport and consumption in the unsaturated zone.'' *J. Hydro.*, Amsterdam, 129(2), 349–369.

Roy, P. (1984). *Coastal geomorphology in Australia*, ''New South Wales estuaries: Their origin and evolution.'' Thom, ed., Academic, San Diego.

Sammut, J., White, I., and Melville, M. (1996). ''Acidification of an estuarine tributary in eastern Australia due to drainage of acid sulphate soils.'' *Marine and Freshwater Res.*, 47(3), 699–684.

Troeh, F., Jabro, J., and Kirkham, D. (1982). ''Gaseous diffusion equations for porous materials.'' *Geoderma*, 27(2), 239–253.

White, I., Melville, M., Sammut, J., and Wilson, B. (1997). ''Reducing acidic discharges from coastal wetlands in eastern Australia.'' *Wetlands Ecology and Mgmt.*, 5(1), 55–72.

Wilson, B., White, I., and Melville, M. (1999). ''Floodplain hydrology, acid discharge, and water quality change associated with drained acid sulfate soil.'' *Marine and Freshwater Res.*, 50, 149–157.

Wunderly, M., Blowes, D., Frind, E., and Ptacek, C. (1996). ''Sulfide mineral oxidation and subsequent reactive transport of oxidation products in mine tailings impoundments: A numerical model.'' *Water Resour. Res.*, 32(10), 3173–3187